

Fitting Single Particle Energies in *sdgh* Major Shell

Erdal Dikmen and Oğuz Öztürk

Department of Physics, Süleyman Demirel University, 32260 Isparta, Turkey

Yavuz Cengiz

*Department of Electronics and Communication Engineering,
Süleyman Demirel University, 32260 Isparta, Turkey*

(Dated: January 21, 2021)

We have performed two kinds of non-linear fitting procedures to the single-particle energies in the *sdgh* major shell to obtain better shell model results. The low-lying energy eigenvalues of the light Sn isotopes with $A = 103 - 110$ in the *sdgh*-shell are calculated in the framework of the nuclear shell model by using CD-Bonn two-body effective nucleon-nucleon interaction. The obtained energy eigenvalues are fitted to the corresponding experimental values by using two different non-linear fitting procedures, i.e., downhill simplex method and clonal selection method. The unknown single-particle energies of the states $2s_{1/2}$, $1d_{3/2}$, and $0h_{11/2}$ are used in the fitting methods to obtain better spectra of the $^{104,106,108,110}\text{Sn}$ isotopes. We compare the energy spectra of the $^{104,106,108,110}\text{Sn}$ and $^{103,105,107,109}\text{Sn}$ isotopes with/without a nonlinear fit to the experimental results.

PACS numbers: 21.60.Cs, 21.10.-k, 21.60.Fw

I. INTRODUCTION

The nuclear shell model assumes any nuclei as a many-body quantum mechanical system specified by the Hamiltonian in the second quantization

$$H = \sum \epsilon_{\alpha} a_{\alpha}^{\dagger} a_{\alpha} + \sum V_{\alpha\beta\gamma\delta}^{eff} a_{\alpha}^{\dagger} a_{\beta}^{\dagger} a_{\delta} a_{\gamma} \quad (1)$$

The solution of this Hamiltonian for a series of nuclei in the periodic table implies deriving systematically some nuclear properties such as the energy spectra, electromagnetic transitions, and beta decay, etc [1, 2].

The quantum many-body solution of the Hamiltonian in Eq. (1) for a series of nuclei is very complex that is normally divided in two sub-problems: the first one being the establishment of an effective interaction V^{eff} from the bare nucleon-nucleon (NN) potential in a valence space and of a set of valence space single-particle energies for sequences of nuclei. The second problem is the quantum many-body calculations of the Hamiltonian in Eq. (1) [3]. In this article, we present an improvement under the first problem.

The one-body part of the Hamiltonian in Eq. (1), i.e., the first term, describes the interaction of the valence nucleons with the closed core. The second term is the two-body part which describes the two-body effective interaction. In this study we have used the CD-Bonn two-body effective interactions in the *sdgh*-shell provided to us by M. Hjorth-Jensen et al. [4]. They calculate the charge-dependent Bonn (CD-Bonn) two-body effective interaction V^{eff} for shell model studies based on the free nucleon-nucleon interaction V [5–7]. However, the single-particle energies can not be obtained via their procedure. The latter are normally taken from the experimental data on the nuclei one particle away from the closed shell nuclei. Unfortunately, in the *sdgh* major shell, the nuclei one particle away from the closed shell nucleus ^{100}Sn have

so far escaped by measurements. Therefore, we used instead the single-particle energies for neutrons in the *sdgh* major shell in our earlier studies around $A = 100$ mass region [8–13], e.g., $\epsilon_{1d_{5/2}} = 0.00$ MeV, $\epsilon_{0g_{7/2}} = 0.08$ MeV, $\epsilon_{2s_{1/2}} = 2.45$ MeV, $\epsilon_{1d_{3/2}} = 2.55$ MeV, and $\epsilon_{0h_{11/2}} = 3.20$ MeV. These energies are in reasonable agreement with similar shell model calculations in this region, see for example Ref. [14–16]. However, in the recent experimental work of Ref. [17] an excited state at 171.7 keV has been identified in ^{101}Sn and interpreted as the $0g_{7/2}$ single-neutron state.

The experiment in Ref. [17] fixes the ambiguity about the single-particle energy of the $0g_{7/2}$ orbit. So, the uncertain single-particle energies in the *sdgh* major shell are left only on three of them, namely $\epsilon_{2s_{1/2}}$, $\epsilon_{1d_{3/2}}$, and $\epsilon_{0h_{11/2}}$. The ambiguity of these single-particle energies establishes the need of this work. In this work, we have performed two kinds of non-linear fitting methods, namely downhill simplex method and clonal selection principle, to obtain the optimum single-particle energies for the single-particle orbits of $2s_{1/2}$, $1d_{3/2}$, and $0h_{11/2}$.

In order to obtain a better energy spectrum of any isotopes in *sdgh* major shell in the nuclear shell model framework we should improve both the two-body effective interactions and the single-particle energies given in Eq. (1). Wildenthal in Ref. [18] provided a fit procedure in the *sd*-shell whereby be improved on an effective interaction by fitting the 3 single-particle energies and 63 effective two-body matrix elements. The question being considered in that study is: What is the best possible shell model description of the nuclei in the *sd*-shell independently of what the Hamiltonian is? The same ambitious question was raised by Honma *et al.* [19] for the *pf*-shell, where there are 4 single-particle energies and 195 effective two-body matrix elements to fit.

In the *sdgh*-shell there are 5 single-particle energies

and 542 two-body matrix elements of effective interaction V^{eff} that specifies the Hamiltonian. A global fit of both the single-particle energies and these two-body matrix elements is certainly out of question. Many of the *sdgh*-shell nuclei can not be calculated yet, some of the nuclei that can be modeled require very large calculations and we have limited experimental data. This study restricts itself to fit single-particle energies.

We have five single-particle states in the *sdgh* major shell. All theoretical and experimental data indicate that the lowest single-particle state is the $1d_{5/2}$ state and the energy of the $0g_{7/2}$ state are experimentally known [4, 5, 8–17]. So we fix the $1d_{5/2}$ state as the lowest at the energy of 0.00 MeV and the $0g_{7/2}$ state as the first excited state at the energy of 0.172 MeV, and then perform a non-linear fit to the other three single-particle energies. We use the downhill simplex method [20] and the clonal selection principle [21] in three dimensions to fit these three unknown single-particle energies. The downhill simplex method was chosen over the others, i.e., steepest decent annealing, monte carlo, because of the claim that it avoids trapping in local minima. The clonal selection principle was chosen because it represents a global fit over the all cells.

II. FITTING SINGLE PARTICLE ENERGIES IN 3-D

Because of the complexity and very large model space of the two-body effective interaction in the *sdgh* major shell, we only apply a fit process to the values of the single-particle energies. We adjust the values of the single-particle energies so as to fit the theoretical energy levels of the selected nuclei to the experimental energy levels. We outline some major steps in the present study and the fitting procedures below.

For a set of known experimental energy data $E_{exp}^J (J = J_1, J_2, \dots)$ with the angular momentum J of a specific nucleus with a mass A , we calculate corresponding shell-model energy eigenvalues E_J^{theory} . We minimize the quantity

$$\sigma^2 = \sum_A \sum_{J=J_1, J_2, \dots} (E_{exp}^J - E_{theory}^J)^2 \quad (2)$$

by varying the values of the single-particle energies. Since the fitting methods that we use, simplex and clonal selection, are the non-linear processes with respect to the parameters, it is solved in an iterative way with successive variations of those parameters (single-particle energies) followed by diagonalization of the Hamiltonian until convergence.

We choose the light even-even Tin isotopes experimentally available. Since the fit process is a non-linear process, the selection of the heavier nuclei would require very long calculation times until convergence. Therefore the nuclei $^{104,106,108,110}\text{Sn}$ are the largest Tin isotopes for

which we can fit the single-particle energies in some reasonable time. On the other hand, the more number of nuclei are included in the fit process, the more accurate fitted single-particle energies are obtained in the *sdgh* major shell.

There are 5 single-particle energies in *sdgh*-shell model space. For simplicity we reduce the dimension of the problem to 3-D instead of 5-D by fixing the energies of the $1d_{5/2}$ state to be 0.000 MeV and the $0g_{7/2}$ state to be 0.172 MeV. The energy values of the other three single-particle states $2s_{1/2}$, $1d_{3/2}$, and $0h_{11/2}$ are varied during fitting process. The experimental energies used for the fit are limited to those of the first occurrences of low-lying states. The theoretical energies are also chosen to be the lowest in the theoretical spectra.

A. The Downhill Simplex Method in Multidimensions

The downhill simplex method is a geometrical hill climbing scheme to find the minimum of a function of more than one independent variable. The method requires only function evaluations. A simplex is a geometrical figure with $N + 1$ points (or vertices) that lives in a parameter space of dimension N and all interconnecting line segments and polygonal faces of vertices. In 2-D space a simplex is a triangle, in 3-D space it is a tetrahedron, and so on. Given the function value at each of the simplex's vertices, the worst vertex is displaced by having the simplex undergo one of four possible “moves”, namely reflection, reflection and expansion, contraction, or multiple contraction (see more details in Ref. [20, 22]).

The downhill simplex method starts with $N + 1$ points defining an initial simplex. If one of $N + 1$ points is the initial starting point P_0 , then the other N points are

$$P_i = P_0 + \lambda e_i \quad (3)$$

where e_i 's are N unit vectors, and λ is a constant characterizing the problem's length scale (or λ may be different on each direction).

The downhill simplex method takes a series of moves, most moves just moving the point of the simplex where the function is largest (“highest point”) through the opposite face of the simplex to a lower point. These moves are called reflections, and they are constructed to conserve the volume of the simplex. When it can do so, the method expands the simplex in one or another direction to take larger moves. When it reaches a “valley floor” the simplex contracts itself in the transverse direction and tries oozing down the valley. If there is a situation where the simplex is trying to “pass through the eye of a needle” it contracts itself in all directions, pulling itself in around its lowest (best) point. The simplex undergoes successive such moves until no move can be found that leads to further improvement beyond some present tolerance.

The simplex method requires that one provides initial coordinates (x,y) for the simplex's four vertices. Despite the simplex method's pseudo-global abilities on a multi-dimensional and global problem, the choice of the initial location for the simplex often determines whether the global maximum or minimum is ultimately found.

B. The Clonal Selection Principle

Artificial Immune Systems (AIS) are computational methods inspired by biological principles of the natural immune system. AIS uses the ideas from immunology to develop an algorithm describing adaptive systems in various areas of science and engineering applications [23, 24]. The clonal selection algorithm is based on the idea of AIS and focuses on a systematic view of the immune system. The algorithm is initially proposed to carry out machine-learning and pattern-recognition tasks and then is applied to optimization problems [24]. In the optimization problems, this algorithm uses random instead of certain passing rules to avoid sticking on a local minima.

Clonal selection algorithm uses two kinds of populations of strings: a set of antigens (corresponding to a objective function) and a set of antibodies (corresponding to variables of the objective function) within the maximum and minimum limits of variables. Antibody population is generated by random numbers scaled by limits of variables. The affinity value of an antibody matches the value of purpose function calculated for a given antibody. The affinity population matrix is obtained by sorting affinity values. The amount of antibodies having highest affinity are selected from the entire population and a new set of population is formed as a sub-antibody array.

A cloning ratio is determined by a percentage of each antibody array elements. Each of antibody array elements is cloned by cloning ratio and inverting cloning factor determining the number of cloning. The affinity values of the new cloned population exposed to mutation are calculated and then a hypermutation process is performed by inverse cloning ratio. After the hypermutation process, a new number of antibody are determined and the cloned antibody array is obtained by sorting the corresponding affinity values. An amount of antibodies with highest affinity are reselected and added to the antibody population set. Finally, an amount of antibodies with low affinity value within the antibody population set are replaced with the newly formed antibodies. At the end, the optimum values are determined.

III. RESULTS AND DISCUSSION

The initial values of the single-particle energies to be fitted are chosen to be $\varepsilon_{2s_{1/2}} = 2.45$ MeV, $\varepsilon_{1d_{3/2}} = 2.55$ MeV, and $\varepsilon_{0h_{11/2}} = 3.20$ MeV. These energies are in reasonable agreement with similar shell model calculations in this region [8–16].

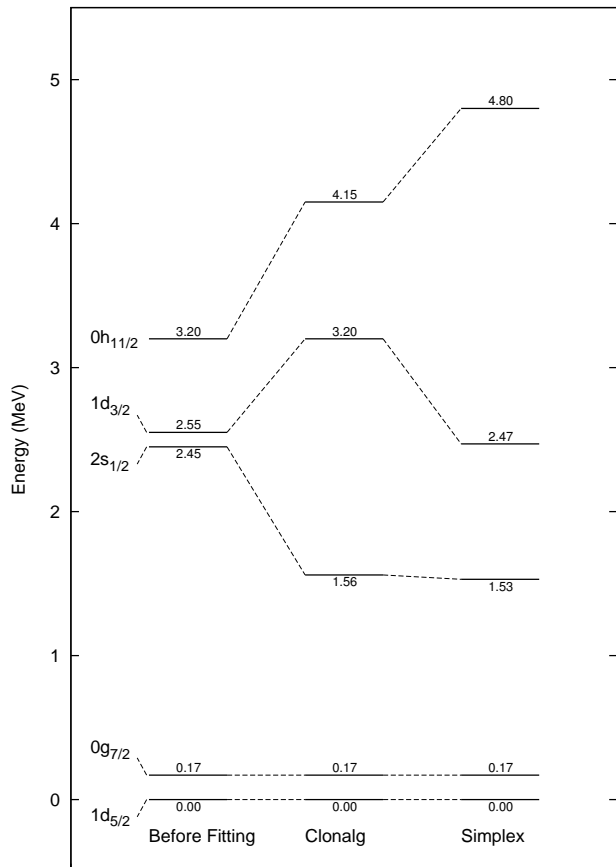


FIG. 1: The single-particle energies before and after the fit processes.

The calculation time for each iteration in both simplex and clonal selection fitting methods is very long time since it requires the shell-model calculations of the states $J^\pi = 0^+, 2^+, 4^+, 6^+, 8^+, 10^+$ for the Tin isotopes $^{104,106,108,110}\text{Sn}$. We have carried out the shell-model calculations in the High Performance Parallel Computer Cluster at Suleyman Demirel University, Turkey, consisting of 1 master and 30 slave nodes with each one of 3.2 GHz Dual Xeon Processors. For a comparison, the required time to calculate the energy of the state 4^+ of ^{108}Sn and ^{110}Sn are about 10 min. and 156 min., respectively. The largest Hamiltonian dimension among the states that we include in the fitting process is 156674 for the state 8^+ of ^{110}Sn .

The fitted single-particle energies obtained by using clonal selection algorithm and simplex algorithm are shown in Figure 1 as compared to the ones before fitting. As mentioned above, the energies of the single-particle states $1d_{5/2}$ and $0g_{7/2}$ are fixed to the values of 0.00 MeV and 0.17 MeV, respectively. Both fits give almost same fitted energy of the single-particle state $2s_{1/2}$ to be 1.56 MeV and 1.53 MeV by lowering almost 1 MeV from the initial value of 2.45 MeV. The energies of the

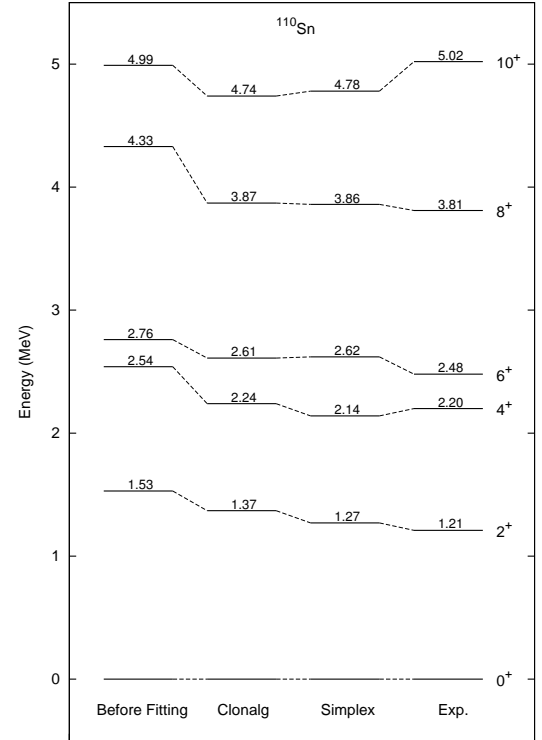
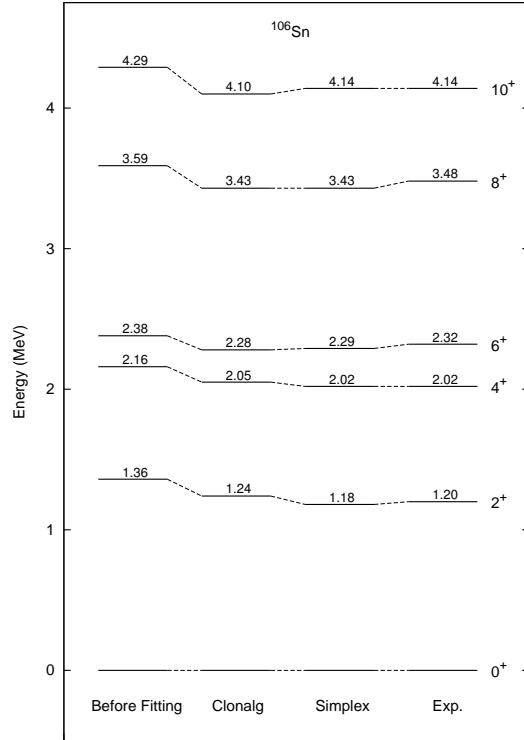
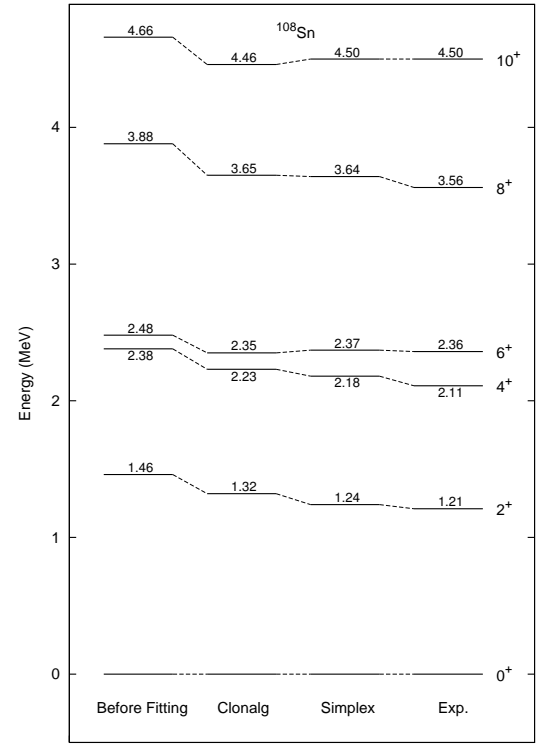
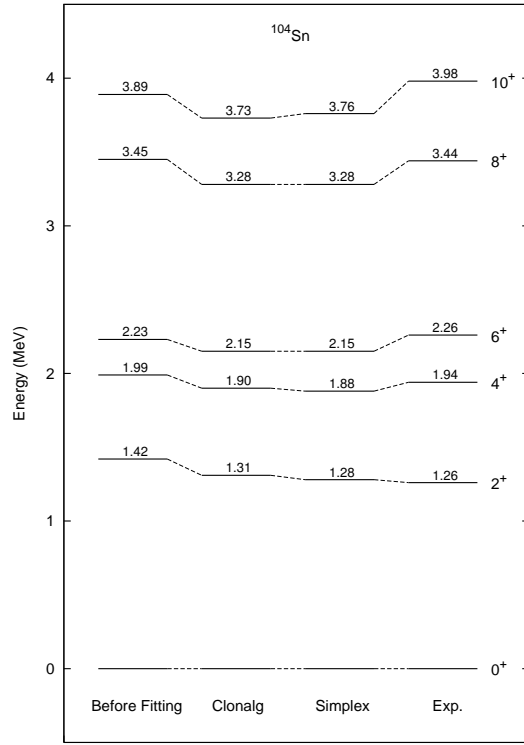


FIG. 2: Experimental and theoretical spectrum of ^{104}Sn and ^{106}Sn obtained with the single-particle energies before fit and the fitted ones using the CD-Bonn effective interaction.

FIG. 3: Experimental and theoretical spectrum of ^{108}Sn and ^{110}Sn obtained with the single-particle energies before fit and the fitted ones using the CD-Bonn effective interaction.

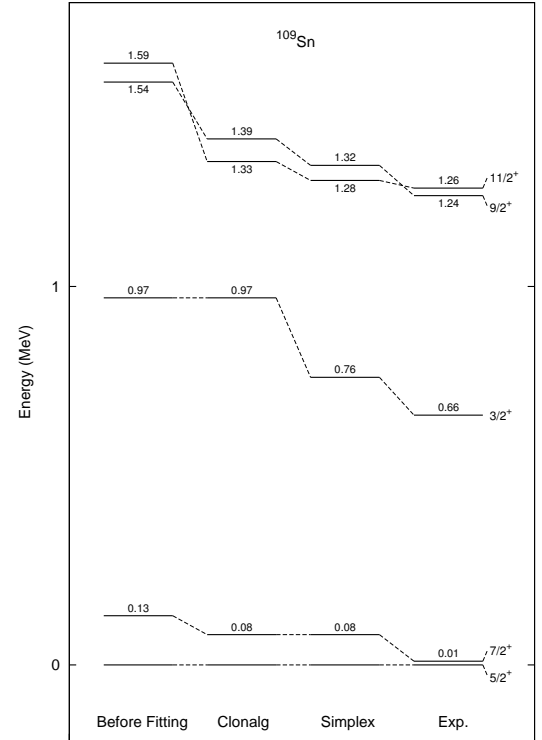
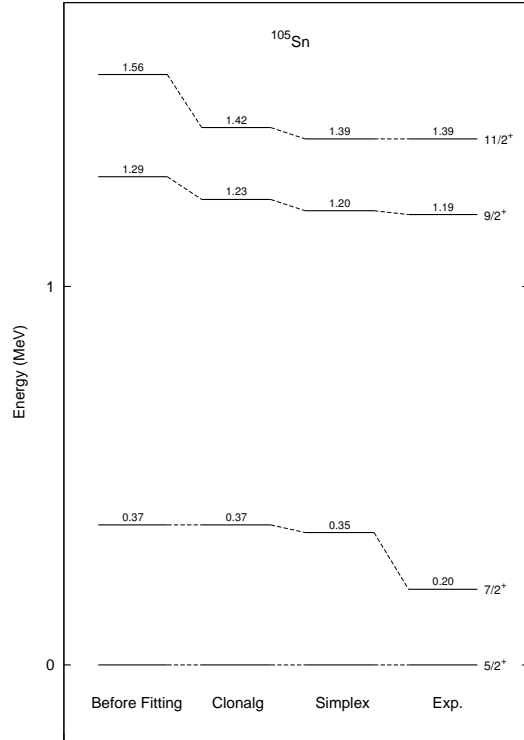
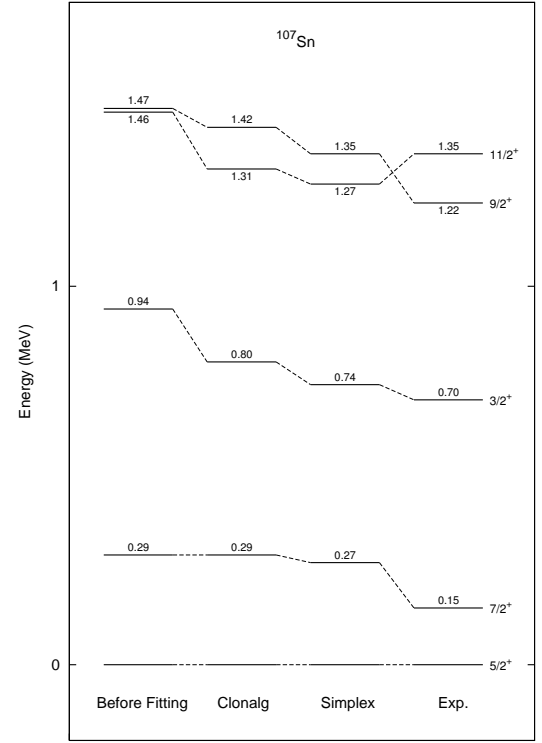
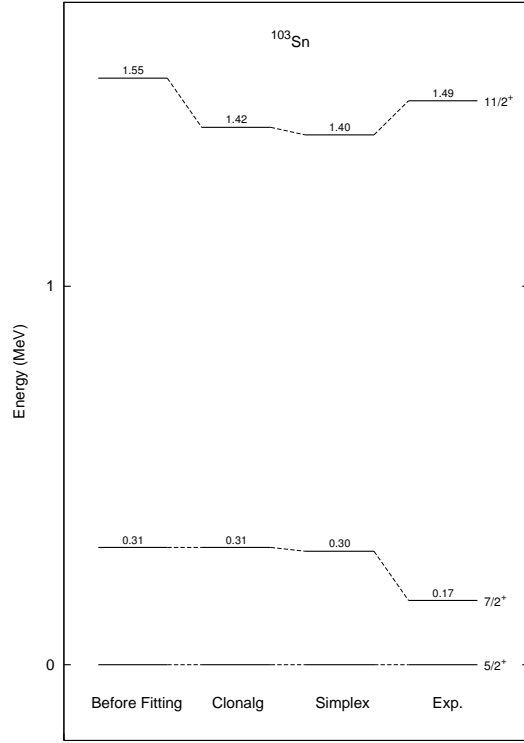


FIG. 4: Experimental and theoretical spectrum of ^{103}Sn and ^{105}Sn obtained with the single-particle energies before fit and the fitted ones using the CD-Bonn effective interaction.

FIG. 5: Experimental and theoretical spectrum of ^{107}Sn and ^{109}Sn obtained with the single-particle energies before fit and the fitted ones using the CD-Bonn effective interaction.

TABLE I: The σ , root mean square (rms), values for the 2^+ , 4^+ , 6^+ , 8^+ , 10^+ states of Sn isotopes with $A = 104-110$ before and after fitting processes.

A Sn	J_i^π	σ_{before}	σ_{clonal}	σ_{simplex}
^{104}Sn	2^+	0.16	0.05	0.02
	4^+	0.05	0.04	0.06
	6^+	0.03	0.11	0.11
	8^+	0.01	0.16	0.16
	10^+	0.09	0.25	0.22
^{106}Sn	2^+	0.16	0.04	0.02
	4^+	0.14	0.03	0.00
	6^+	0.06	0.04	0.03
	8^+	0.11	0.05	0.05
	10^+	0.15	0.04	0.00
^{108}Sn	2^+	0.25	0.11	0.03
	4^+	0.27	0.12	0.07
	6^+	0.12	0.01	0.01
	8^+	0.32	0.09	0.08
	10^+	0.16	0.04	0.00
^{110}Sn	2^+	0.32	0.16	0.06
	4^+	0.34	0.04	0.06
	6^+	0.28	0.13	0.14
	8^+	0.52	0.06	0.05
	10^+	0.03	0.28	0.24

other two single-particle states $1d_{3/2}$ and $0h_{11/2}$ are very different each other after the fit processes. The simplex method changes the energy of the single-particle state $1d_{3/2}$ -0.008 MeV as to be 2.47 from the initial value of 2.55 MeV while clonal selection method makes the change +0.65 MeV as to be 3.20 MeV. The major change happens to the energy of the single-particle state $0h_{11/2}$: with a change of +0.95 MeV and +1.6 MeV along with clonal selection and simplex methods, respectively.

As we mentioned in Section II, the convergence of optimization algorithms are satisfied by minimizing the quantity, σ^2 , given in Eq. (2). The value of σ^2 before fitting process is 1.127. The values of σ^2 after fitting processes are 0.208 after 76 iterations for simplex algorithm and 0.256 after 130 iterations for clonal selection algorithm. Both simplex and clonal selection algorithms quit the iterations by having unchange value of σ^2 , 0.208 and 0.256 respectively. Therefore, the convergence of the fitted single-particle energies are obtained by lowering the value of σ^2 from 1.127 to 0.208 and 0.256 for simplex and clonal selection methods, respectively.

After having the fitted single-particle energies, we have carried out the shell-model calculations for the states 0^+ , 2^+ , 4^+ , 6^+ , 8^+ , 10^+ of even-even $^{104,106,108,110}\text{Sn}$ isotopes to see how good spectrum obtained by using the new single-particle energies. In Table I, we have given the root mean square (rms) deviations, σ , i.e., calculated by using Eq. 2, for the states 0^+ , 2^+ , 4^+ , 6^+ , 8^+ , 10^+ of $^{104,106,108,110}\text{Sn}$ to see the goodness of the energy spectra before and after fitting processes.

Figure 2 shows a comparison among the experimental, theoretical and fitted spectra of the ^{104}Sn isotope. Both

fits give very similar energies for the states 0^+ , 2^+ , 4^+ , 6^+ , 8^+ , 10^+ of ^{104}Sn . Both clonal selection and simplex fits improve the energies of the low-spin states 2^+ and 4^+ from 1.42 MeV to 1.31 MeV and 1.28 MeV, from 1.99 MeV to 1.90 MeV and 1.88 MeV, respectively, compare to the experimental data. The energy of the states 6^+ , 8^+ , 10^+ is not improved through the both fits.

Figure 2 also compares theoretical and fitted spectra of the ^{106}Sn isotope to the experimental spectra. All fitted states merge to the experimental ones. The states 4^+ and 10^+ are exactly reproduced by simplex and the states 2^+ , 6^+ , 8^+ are deviated slightly as to be 0.04, 0.04, 0.05 MeV and 0.02, 0.03, 0.05 MeV by clonal selection and simplex methods, respectively. Overall, the simplex methods gives slightly better spectrum with respect to the clonal selection method for the ^{106}Sn isotope.

Figure 3 shows the theoretical (before fitting) and experimental spectra of the ^{108}Sn isotope as well as the fitted ones. From Table I, the energy deviations of the states to the experimental ones are 0.11, 0.03 MeV for 2^+ , 0.12, 0.07 MeV for 4^+ , 0.01, 0.01 MeV for 6^+ , 0.09, 0.08 MeV for 8^+ , and 0.04, 0.00 MeV for 10^+ with clonal selection and simplex methods, respectively. As we see from these rms deviations, all states merge gradually to the corresponding experimental ones. This mergence shows a definite improvement on the spectrum of the ^{108}Sn isotope.

Figure 3 also shows the theoretical (before fitting) and experimental spectra of the ^{110}Sn isotope as well as the fitted ones. All energy levels except the state 10^+ merge to the experimental energies with the rms deviations of 0.16, 0.06 MeV for 2^+ , 0.04, 0.06 MeV for 4^+ , 0.13, 0.14 MeV for 6^+ , 0.06, 0.05 MeV for 8^+ of clonal selection and simplex methods, respectively. Both fit processes do not improve the energy level of the state 10^+ .

If we look at the systematic behavior of the states compare to before and after fitting processes, the states 2^+ and 4^+ are definitely improved with both fitting procedures for all $^{104,106,108,110}\text{Sn}$ isotopes; the states 6^+ and 8^+ are fitted well for the $^{106,108,110}\text{Sn}$ isotopes and not for ^{104}Sn ; the state 10^+ is fitted well for $^{106,108}\text{Sn}$ isotopes and not for $^{104,110}\text{Sn}$ isotopes.

To see the goodness of the obtained single-particle energies we have also carried out the shell-model calculations with the fitted single-particle energies for the lowest states $\frac{3}{2}^+$, $\frac{5}{2}^+$, $\frac{7}{2}^+$, $\frac{9}{2}^+$, $\frac{11}{2}^+$ of the light odd-even $^{103,105,107,109}\text{Sn}$ isotopes. Figures 4 and 5 show such a spectrum comparing the calculated (before fitting) and available experimental values of the states $\frac{3}{2}^+$, $\frac{5}{2}^+$, $\frac{7}{2}^+$, $\frac{9}{2}^+$, $\frac{11}{2}^+$ of the $^{103,105}\text{Sn}$ and $^{107,109}\text{Sn}$ isotopes, respectively, as well as the fitted ones.

In Figure 4, the states $\frac{7}{2}^+$ and $\frac{11}{2}^+$ of ^{103}Sn and $\frac{7}{2}^+$, $\frac{9}{2}^+$, $\frac{11}{2}^+$ of ^{105}Sn are lowered well to get close to the experimental values. The states with higher energies of ^{105}Sn , e.g., $\frac{9}{2}^+$ and $\frac{11}{2}^+$, are fitted better with respect to the lower ones.

In Figure 5 the states $\frac{7}{2}^+$ of ^{107}Sn and ^{109}Sn are fitted

to the values of 0.29 (0.27) and 0.08 (0.08) MeV with the rms deviations of 0.14 (0.12) MeV and 0.07 (0.07) MeV of clonal selection and simplex methods, respectively. The energy of $\frac{3}{2}^+$ state is much better fitted to the corresponding experimental value by lowering about -0.20 MeV. As in the case of ^{105}Sn , the states with higher energies of ^{107}Sn and ^{109}Sn are fitted better with respect to the lower ones.

As we see from the Figure 4 and 5, the fitted spectra of odd-even $^{103,105,107,109}\text{Sn}$ isotopes agree with the experimental data better than the ones of even-even $^{104,106,108,110}\text{Sn}$ isotopes. This is an evidence that the fitted single-particle energies give better spectrum for the other Sn isotopes which are not part of the fitting processes.

IV. CONCLUSION

The non-linear fitting procedures, namely clonal selection and simplex methods, have been applied to optimize the single-particle energies in the *sdgh* major shell in the nuclear shell model calculations. The fitted single-particle energies are calculated as to be $\varepsilon_{2s_{1/2}} = 1.53$ (1.56) MeV, $\varepsilon_{1d_{3/2}} = 2.47$ (3.20) MeV, and $\varepsilon_{0h_{11/2}} = 4.80$ (4.15) MeV with the simplex algorithm (the clonal selection algorithm). The fitted energy of the single-particle state $2s_{1/2}$ are almost the same in both fit processes, but the other two fitted energies of the single-particle states are very different from each other. The optimization ideas of the simplex and clonal selection methods give this difference. The obtained fitted single-particle energies are still in the range of expectation. Indeed, there is a minimum and maximum limits of energy variables within the clonal selection algorithm while there is no limits of variables within the simplex algorithm.

For the point of shell model calculations, we have re-

peated the shell model calculations of the states 0^+ , 2^+ , 4^+ , 6^+ , 8^+ , 10^+ of the $^{104,106,108,110}\text{Sn}$ isotopes with the single-particle energies obtained before and after fitting processes to get better agreement of shell model spectra with the experiment. We have obtained better energy spectra of the $^{104,106,108,110}\text{Sn}$ isotopes with the fitted single-particle energies. The fit processes improve the all states of the $^{104,106,108,110}\text{Sn}$ isotopes except the higher excited states of ^{104}Sn and the state 10^+ of ^{110}Sn . So, the overall agreement of the fitted spectra is very good with experiment.

We have also performed the shell model calculations of the states $\frac{3}{2}^+$, $\frac{5}{2}^+$, $\frac{7}{2}^+$, $\frac{9}{2}^+$, $\frac{11}{2}^+$ of the light odd-even $^{103,105,107,109}\text{Sn}$ isotopes with the single-particle energies obtained before and after fitting processes. We have obtained even better energy spectra for the $^{103,105,107,109}\text{Sn}$ isotopes with respect to the $^{104,106,108,110}\text{Sn}$ isotopes which are parts of the fitting processes.

The fitted single-particle energies with the simplex method give the spectra slightly better corresponding to the experiment with respect to the ones with clonal selection method. The fitted single-particle energies can be used to do the shell model calculations for the other nuclei in the vicinity of ^{100}Sn , especially for mid-heavy Tin (Sn) isotopes with $A = 110 - 120$ and light Antimony (Sb) isotopes. With this study, we present an improvement on the ambiguity of the single-particle energies to be used in future shell model calculations in the *sdgh* major shell.

Acknowledgments

This work was supported in part by Süleyman Demirel University under Contract No. SDUBAP 1822-YL-09 and The Scientific and Technological Council of Turkey under Contract No. TUBITAK 105T092.

-
- [1] I. Talmi, *Simple Models of Complex Nuclei* (Harwood Academic, Switzerland, 1993).
 - [2] Kris L.G. Heyde, *The Nuclear Shell Model* (Springer-Verlag, Germany, 1994).
 - [3] E. Dikmen, Mathematical and Computational Applications **11**, 41 (2006).
 - [4] M. Hjorth-Jensen *et al.*, private communication.
 - [5] M. Hjorth-Jensen, T.T.S. Kuo, E. Osnes, Phys. Rep. **261** 125 (1995).
 - [6] R. Machleidt, F. Sammarruca, Y. Song, Phys. Rev. C **53** R1483 (1996).
 - [7] R. Machleidt, Phys. Rev. C **63** 024001 (2001).
 - [8] E. Dikmen, A. Novoselsky, and M. Vallieres, Phys. Rev. C **64**, 067305 (2001).
 - [9] E. Dikmen, A. Novoselsky, and M. Vallieres, Phys. Rev. C **66**, 057302 (2002).
 - [10] E. Dikmen, Chin. Phys. Lett. **23**, 1430 (2006).
 - [11] E. Dikmen, A. Novoselsky, and M. Vallieres, J. Phys. G: Nucl. Part. Phys. **34**, 529 (2007).
 - [12] E. Dikmen, Commun. Theor. Phys. **51**, 899 (2009).
 - [13] E. Dikmen, O. Ozturk, and M. Vallieres, J. Phys. G: Nucl. Part. Phys. **36**, 045102 (2009).
 - [14] Andreozzo, F., et al., Phys. Rev. C **56**, R16 (1997).
 - [15] T. Engeland, M. Hjorth-Jensen, and E. Osnes, Phys. Rev. C **61**, 021302(R) (2000).
 - [16] T. Engeland, M. Hjorth-Jensen, and E. Osnes, Nucl. Phys. A **701**, 2002 (2002).
 - [17] D. Seweryniak *et al.*, Phys. Rev. Lett. **99**, 022504 (2007).
 - [18] B.H. Wildenthal, Prog. Part. Nucl. Phys. **11**, 5 (1984).
 - [19] M. Honma, T. Otsuka, B.A. Brown, and T. Mizusaki, Phys. Rev. C **65**, 061301 (2002).
 - [20] J.A. Nelder, and R. Mead, Computer Journal **7**, 308 (1965).
 - [21] Leandro N. de Castro, IEEE T. Evolut. Comput. **6** 239 (2002).
 - [22] W.H. Press, S.A. Teukolsky, W.T. Vetterling, and B.P.

- Flannery, Numerical Recipes, Second Edition, Cambridge University Press, U.S.A. (1992).
- [23] H.S. Bernardino, H.J.C. Barbosa, Nature-Inspired Algorithms for Optimisation, Studies in Computational Intelligence **193**, 389 (2009).
- [24] L.N. de Castro and F.J. Von Zuben, IEEE Transactions on Evolutionary Computation **6**, 239 (2002).